Adaptive Sliding Mode Control Analysis of Non-Linear TB Epidemic Model

Rabiu Aliyu Abdulkadir[1], Bashir Abdullahi Baba[2], Usman Aliyu Magaji[1], Shamsu Idris Abdullahi[3] Abdullahi Garba Musa[1]

[1]Department of Electrical Engineering, Faculty of Engineering, Aliko Dangote University of Science and Technology, P.M.B. 3244, Wudil, Kano, Nigeria

[2]Department of Computer Science, Sule Lamido University, Kafin Hausa, P.M.B. 048, Jigawa, Nigeria

[3]Department of Electrical Engineering, Kano State Polytechnic, P.M.B. 3401, Kano, Nigeria

ARTICLE INFO

Article History
Received: 16 November 2022
Accepted: 26 July 2023
Published: 19 August 2024

Corresponding Author:
R.A. Abdulkadir
Faculty of Engineering, Aliko Dangote University of Science and Technology, Wudil
rabiu.abdulkadir@kustwudil.edu.ng

ABSTRACT

Designing appropriate control intervention programs for handling infectious diseases such as tuberculosis (TB) involves elongated engagement with complex and challenging tasks. Several researchers used mathematical models and control system theory as a valuable tool in studying infectious disease dynamics and control. However, the majority of the previous studies for TB control are based on open-loop optimal control theory. In the design of the conventional optimal control approach, system parameters are assumed to be prior known and accurate. However, if the system contains uncertain parameters, the conventional control techniques may not provide the desired results. Therefore, in this study a robust adaptive sliding mode control (ASMC) strategy is applied to a non-linear TB model to handle the parameter uncertainties. The control objective is to decrease the population of individuals that are exposed and infected to zero by tracking a predefined reference trajectory. Adaption law is defined to update the parameter values to ensure the robustness of the control system against uncertainties. The stability of the closed-loop system is proved using the Lyapunov Function Theory, and the result is validated through numerical simulations. The study identifies alternative solutions in finding practically useful control strategies and illustrates the essential applications of closed-loop control systems. The work highlights a new methodology to inform realistic approaches towards realizing the United Nations (UN) 2030 plan for eradicating TB disease.

Keywords: *Epidemic Model · TB · Adaptive Control · Sliding Mode Control ·*

1. Introduction

Epidemic diseases such as tuberculosis (TB) have been a contributing cause of billions of deaths in several decades. The entire world is committed to finding effective control and prevention strategies to contain the epidemic outbreak. Several researches used mathematical modelling and control system theory to study the infectious disease dynamics and facilitate the design of control intervention programs to curtail the spread of the diseases [1]–[3]

TB is caused by a bacterial infection that usually starts in the body of a susceptible person (a healthy person that can contract the disease) as a result of infection by Mycobacterium tuberculosis (MTB). The disease is commonly transmitted through the air by the breath of healthy person and infected individuals, and the common symptoms of TB include coughing blood, fever and weight loss [4]. An infected person with MTB may develop active TB or remain latent. Latently infected people are asymptomatic and do not transmit the disease, but may progress to infectious (active TB) after a latency period [5]. TB is treatable and can be cured. Nonetheless, inability to comply with the medication may lead to the emergence of drug-resistant TB [6].

Various control interventions are available for TB prevention and treatment. Vaccination is the most preferred method of treating TB which is used to protect the susceptible individual from contracting the disease and subsequently prevent further dissemination of the infection. Reactivation of TB in an exposed person (latently infected individuals) can be controlled through a control effort known as "case finding", which involves the monitoring action by public health workers to find and treat the exposed individuals to stop them from becoming infectious. Furthermore, the development of drug-resistant TB can be prevented by employing intervention program referred to as "case holding". The case holding control effort represent the interventions made by health workers to ensure adherence to the proper treatment of the infected people [7], [8].

In order to predict the future characteristics of the infectious disease and plan reliable control intervention programs to minimize disease outbreak, a thorough understanding of dynamics of the disease transmission among populations is essential [9]. Mathematical modelling and control theory has been one of the important tools for studying the dynamics and control of infectious disease [10], [11]. Design and control analysis of epidemic models, however, involves a complex and quite challenging process; due to the inherent non-linearity, and parameter uncertainties associated with epidemic processes. This is in addition to the economic constraint of optimizing the demands of the control goals and minimization of the cost of implementing the control actions [12], [13].

Many studies on the mathematical modelling of the dynamics of TB transmission have been performed [14], [15]. However, some of the previous TB predictive models included vaccination and control treatments and analyzed the disease management by evaluating the role of parameters of disease transmission in decreasing the value of the basic reproduction number, R_0, below the threshold limit [15]. Generally, a reproduction number $R_0 < 1$ suggests that the disease is eradicated on its own, while $R_0 > 1$ shows that the disease will persist in the population [16], [17]. These approaches have a major limitation of not taking into consideration the time-dependent control inputs.

Optimal control theory developed from the calculus of variation enables the incorporation of time-dependent control functions, and offers reliable tools to study the time-varying disease control strategies and determines the trade-offs between different control strategies and the cost of implementation. The application of optimal control theory provides the public health authorities with useful suggestions on the impact of one control policy compared to others [18]. Optimal control has been applied in several biomedical problems, especially to cancer chemotherapy models [19], [20]. These methods when implemented to infectious disease models, can offer tremendous insight into the best pathway to reduce disease burden. Many studies have considered the application of optimal control for specific diseases [21]–[24].

Nonetheless, the application of conventional optimal control methods requires that the epidemiological parameters are well known and accurate. This assumption is not always practical because the process of estimating such parameters from experimental data can result in inconsistent values. As a consequence, in the presence of modelling uncertainties and parametric variations, the conventional control techniques can yield unsatisfactory results. Meanwhile, robust and adaptive control techniques which employs feedback will provide more consistent results. The closed-loop control design can achieve the desired control goals irrespective of the model's parameter variations [25]–[27].

Design of control systems, for systems with considerable parameter uncertainty can be approached by adaptive control. Adaptive design methods extract knowledge of the plant parameters online and update the control law. There are several strategies to design adaptive controllers such as $H\infty$, fuzzy, or neural network based techniques [28]–[31]. Among them, sliding-mode control is one of the most well-known technique due to its simple design process, accuracy and reliability.

In this regard, this study focused on the investigation of the application of adaptive control theory for the analysis of TB transmission dynamics, with parameter uncertainties. The rest of the paper is organized as follows: section 2 provides the system model description and parameter definitions. In section 3 the controller

design procedure and the stability analysis of the TB closed-loop control system is explained. The results and discussions are presented in section 4 and the conclusion is discussed in section 5.

2. System Model Description

For this study, an SEI type compartmental nonlinear TB model proposed by [32] is considered. The model transfer diagram is illustrated in Figure 1. In the transfer diagram S, E, and I, respectively, represent the group of the susceptible, exposed and infectious people. The dynamical model is therefore given by the following system of ordinary differential equations (ODEs).

$$\dot{\mathrm{S}} = \Lambda - \beta SI - \mu S \quad (1)$$

$$\dot{\mathrm{E}} = (1-p)\beta SI - aE - \mu E - u_1(\mathrm{t})\mathrm{E} \quad (2)$$

$$\dot{I} = p\beta SI + aE - (d+\mu)\mathrm{I} - u_2(\mathrm{t})\mathrm{I} \quad (3)$$

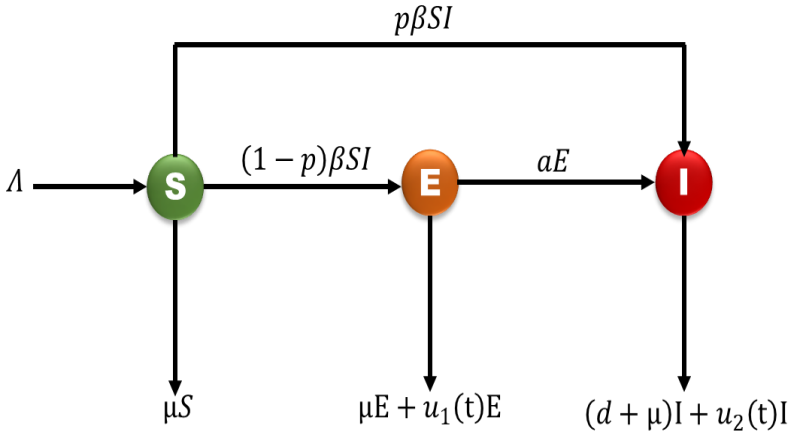

Figure 1. Model transfer diagram

The description of the model's parameters is given in Table 1. The system contains three state variables S, E and I representing the number of susceptible, exposed and infected individuals, respectively, along with their initial conditions $S_0 = S(0), E_0 = E(0)$ and $I_0 = I(0)$. The exposed group comprises of individuals that were in contact with contagious persons but did not reveal any symptoms of infection. A fraction of the exposed group is eliminated through successful chemoprophylaxis or by natural death, while others are transferred into the infectious compartment. In the infectious compartment, there are people who got infected with active TB and can infect others. The population is assumed to be homogeneous with equal natural death rate (μ). The control signal $u_1(t)$ is the rate of case finding control scheme that detects and treats a fraction of individual exposed, while $u_2(t)$ is the control initiative that guarantees successful treatment of individuals infected. The control inputs seek to reduce the population of individuals that are exposed and infected with the TB (hence appeared in Equations (2) and (3)).

Table 1. Parameter description [32]

Parameter Symbol	Parameter description
Λ	Overall recruitment into susceptible compartment
μ	Natural death rate
D	Disease induced death rate
β	Disease transmission coefficient
p	The proportion of newly infected individuals that undergo fast progression to the infectious class
a	The rate at which exposed individuals move to the infectious compartment

3. Controller Design

This section explains the Adaptive Sliding Mode Controller (ASMC) design procedure, starting with the ASMC architecture, followed by the controller design, and the Lyapunov stability analysis of the closed-loop TB controlled system.

3.1 ASMC Architecture

The structure of ASMC for the non-linear TB model is illustrated in Figure 2. The closed-loop control system consists of the ASMC block, the TB model and adaptation laws. By setting appropriate control signals u_1 and u_2, the ASMC controller regulates the values of the state variables. The ASMC is capable of handling both model uncertainties and external disturbances effectively. The TB model contains uncertain parameters due to the discrepancies that occur in different communities. The adaptation laws are included for updating the controller gains in order to maintain the system stability and keep the system response close to the desired conditions despite the presence of the uncertainties.

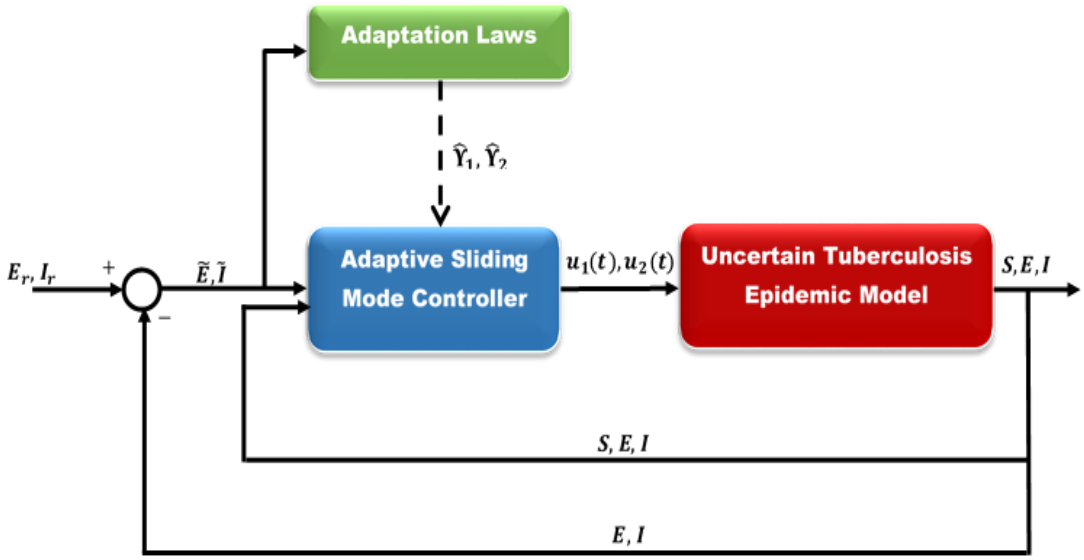

Figure 2. Structure of ASMC for the non-linear TB model

The control objectives are said to be achieved when the actual population of the exposed and infected groups (E *and* I) accurately track a predefined desired reference trajectory ($E_r \to 0$ *and* $I_r \to 0$). In order to realize the control objectives, this implies that the tracking error should be zero for all the time during the process. That is,

$$e(t) = 0, \quad \forall\, t \geq 0,$$
$$\tilde{E} = E - E_r = 0,$$
$$\tilde{I} = I - I_r = 0.$$

In which $\tilde{E}$ and $\tilde{I}$ denotes the tracking error of exposed and infected individuals, accordingly. Also, E_r and E, and I_r and I represent the desired and actual number of exposed and infected populations, respectively.

3.2 ASMC Design

Consider a sliding variable $\Theta(t)$ with integral term [33]:

$$\Theta(t) = e(t) + \phi \int_0^t e(\tau)d\tau \tag{4}$$

The sliding surface that guarantee the controller objectives is given as

$$\Theta(t) = e(t) + \phi \int_0^t e(\tau)d\tau = 0 \tag{5}$$

Where ϕ is a positive sliding surface constant gain, and the time derivative of the sliding surface is given by

$$\dot{\Theta}(t) = \dot{e}(t) + \phi e(t) \quad (6)$$

The characterization of the case finding $u_1(\mathrm{t})$ control input that guarantee the control of the exposed individuals can be written as

$\dot{\Theta}(t) = \dot{\mathrm{E}} - \dot{E}_r + \phi_1(E - E_r) = 0$

substituting the dynamics of exposed E from Equation (2),

$\dot{\Theta}(t) = (1-p)\beta SI - aE - \mu E - u_1(\mathrm{t})\mathrm{E} - \dot{E}_r + \phi_1(E - E_r)$

the case finding $u_1(\mathrm{t})$ control input is obtained as:

$$u_1(t) = -\frac{\left(\dot{E}_r - \phi_1(E-E_r)\right)}{E} - \frac{(1-p)\beta SI}{E} - a - \mu \quad (7)$$

Similarly, the characterization of the case holding $u_2(\mathrm{t})$ control input that guarantee the control of the infected individuals can be written as

$\dot{\Theta}(t) = \dot{\mathrm{I}} - \dot{I}_r + \phi_2(I - I_r) = 0$

Substituting the dynamics of infected I from Equation (3),

the case holding $u_2(\mathrm{t})$ control input is obtained as:

$$u_2(\mathrm{t}) = -\frac{\left(\dot{I}_r - \phi_2(I-I_r)\right)}{I} + p\beta S + a\frac{E}{I} - d - \mu \quad (8)$$

In pursuance of designing the adaptive control law, control inputs (7) and (8) will be express in terms of a matrix $\boldsymbol{X}$ and a vector $\boldsymbol{\theta}$ containing the state variables and the parameters of the system, respectively.

$$u_1(t) = -\frac{\left(\dot{E}_r - \phi_1(E-E_r)\right)}{E} + \boldsymbol{X_1}(S,\, E,\, I)\boldsymbol{\theta_1} \quad (9)$$

$$u_2(\mathrm{t}) = -\frac{\left(\dot{I}_r - \phi_2(I-I_r)\right)}{I} + \boldsymbol{X_2}(S,\, E,\, I)\boldsymbol{\theta_2} \quad (10)$$

Where, $\boldsymbol{X_1}$ and $\boldsymbol{X_2}$ are functions of system states variable $S,\, E\ and\ I$. While, $\boldsymbol{\theta_1}$ and $\boldsymbol{\theta_2}$ contain the uncertain parameters of the system. Accordingly, $\boldsymbol{X_1}$, $\boldsymbol{X_2}$, $\boldsymbol{\theta_1}$ and $\boldsymbol{\theta_2}$ are defined as

$\boldsymbol{X_1} = \left[\frac{SI}{E} \;\; -1 \;\; -1\right]$

$\boldsymbol{X_2} = \left[S \;\; \frac{E}{I} \;\; -1 \;\; -1\right]$

$\boldsymbol{\theta_1} = [(1-p)\beta \;\; a \;\; \mu]^T$

$\boldsymbol{\theta_2} = [p\beta \;\; \kappa \;\; a \;\; \mu]^T$

Furthermore, since the actual system parameters $\boldsymbol{\theta_1}$ and $\boldsymbol{\theta_2}$ contain uncertainties, and the ASMC control laws are therefore designed using estimated model parameters $\widehat{\boldsymbol{\theta}}_{\boldsymbol{1}}$ and $\widehat{\boldsymbol{\theta}}_{\boldsymbol{2}}$, and adaptive laws that handle the mismatch between the actual and estimated parameters [34]:

$$u_1(\mathrm{t}) = -\frac{(\dot{E}_r - \phi_1\tilde{E})}{E} + \boldsymbol{X_1}(S,\, E,\, I)\hat{\theta}_1 + \widehat{\Upsilon}_1\frac{sgn(\tilde{E})}{E} \quad (11)$$

$$u_2(\mathrm{t}) = -\frac{(\dot{I}_r - \phi_2\tilde{I})}{I} + \boldsymbol{X_2}(S,\, E,\, I)\hat{\theta}_2 + \widehat{\Upsilon}_2\frac{sgn(\tilde{I})}{I} \quad (12)$$

Where the vectors $\widehat{\boldsymbol{\theta}}_{\boldsymbol{1}}$ and $\widehat{\boldsymbol{\theta}}_{\boldsymbol{2}}$ denotes the estimated parameters, given by

$$\widehat{\boldsymbol{\theta}}_{\boldsymbol{1}} = \left[(1-\hat{p})\hat{\beta} \;\; \hat{a} \;\; \hat{\mu}\right]^T \quad (13)$$

$$\widehat{\boldsymbol{\theta}}_{\boldsymbol{2}} = \left[\hat{\mathrm{p}}\hat{\beta} \;\; \hat{\mathrm{a}} \;\; \hat{d} \;\; \hat{\mu}\right]^T \quad (14)$$

The adaptation gains $\widehat{\Upsilon}_1$ and $\widehat{\Upsilon}_2$ are included to compensate the discrepancies between estimated and actual parameters so as to attain the control objectives. The adaptation gains are updated through the adaptation laws, defined as [35]:

$$\dot{\widehat{\Upsilon}}_1 = \kappa_1\left|\tilde{E}\right|, \qquad \widehat{\Upsilon}_1(0) = \Upsilon_{10} > 0 \quad (15)$$

$$\dot{\widehat{\Upsilon}}_2 = \kappa_2\left|\tilde{I}\right|, \qquad \widehat{\Upsilon}_2(0) = \Upsilon_{20} > 0 \quad (16)$$

The positive constants κ_1 and κ_2 signifies the rate at which the adaptation gains are updated in reference to the tracking errors $\left(\tilde{E}\ and\ \tilde{I}\right)$. While $\widehat{\Upsilon}_{10}$ and $\widehat{\Upsilon}_{20}$ represent the initial values of the adaptation gain.

3.3 TB Closed-loop Controlled System

The TB closed-loop controlled system is established by using the ASMC designed in sub-section 3.1. In this regard, the control laws (11) and (12) are substituted into dynamics of E and I in Equations (2) and (3), respectively.

$$-\frac{(\dot{\mathrm{E}} - \dot{E}_r + \phi_1\tilde{E})}{E} = \left(1 - (\hat{p} - p)\right)\left(\hat{\beta} - \beta\right)\frac{SI}{E} - (\hat{a} - a) - (\hat{\mu} - \mu) + \widehat{\Upsilon}_1\frac{sgn(\tilde{E})}{E}$$

$$-\frac{(\dot{\mathrm{I}} - \dot{I}_r + \phi_2\tilde{I})}{I} = (\hat{p} - p)\left(\hat{\beta} - \beta\right)S + (\hat{a} - a)\frac{E}{I} - \left(\hat{d} - d\right) - (\hat{\mu} - \mu) + \widehat{\Upsilon}_2\frac{sgn(\tilde{I})}{I}$$

Subsequently, the closed-loop dynamics are obtained as

$$\dot{\tilde{E}} = -\phi_1\tilde{E} - E\boldsymbol{X_1}(S,\, E,\, I)\tilde{\theta}_1 - \widehat{\Upsilon}_1 sgn\left(\tilde{E}\right) \quad (17)$$

$$\dot{\tilde{I}} = -\phi_2\tilde{I} - I\boldsymbol{X_2}(S,\ E,\ I)\tilde{\theta}_2 - \hat{\Upsilon}_2 sgn(\tilde{I}) \quad (18)$$

Where $\dot{\tilde{E}}$ and $\dot{\tilde{I}}$ are the derivatives of the tracking errors, while $\widetilde{\boldsymbol{\theta}}_{\boldsymbol{1}}$ and $\widetilde{\boldsymbol{\theta}}_{\boldsymbol{2}}$ represent the bounded model parameter estimation errors defined as

$\dot{\tilde{E}} = \dot{E} - \dot{E}_r$

$\dot{\tilde{I}} = \dot{I} - \dot{I}_r$

$\widetilde{\boldsymbol{\theta}}_{\boldsymbol{1}} = \widehat{\boldsymbol{\theta}}_{\boldsymbol{1}} - \boldsymbol{\theta}_{\boldsymbol{1}}$

$\widetilde{\boldsymbol{\theta}}_{\boldsymbol{2}} = \widehat{\boldsymbol{\theta}}_{\boldsymbol{2}} - \boldsymbol{\theta}_{\boldsymbol{2}}$

Now, owing to the fact that the system state variables $(S,\ E,\ I)$ and model parameter estimation errors ($\widetilde{\boldsymbol{\theta}}_{\boldsymbol{1}}$ and $\widetilde{\boldsymbol{\theta}}_{\boldsymbol{2}}$**)** are bounded, one can establish that the terms $E\boldsymbol{X_1}(S,\ E,\ I)\widetilde{\boldsymbol{\theta}}_{\boldsymbol{1}}$ and $I\boldsymbol{X_2}(S,\ E,\ I)\widetilde{\boldsymbol{\theta}}_{\boldsymbol{2}}$ are bounded (see [34]), and therefore there exist some positive constants ε_1 and ε_2 such that:

$$\left|E\boldsymbol{X_1}(S,\ E,\ I)\widetilde{\boldsymbol{\theta}}_{\boldsymbol{1}}\right| \leq \varepsilon_1 \quad (19)$$

$$\left|I\boldsymbol{X_2}(S,\ E,\ I)\widetilde{\boldsymbol{\theta}}_{\boldsymbol{2}}\right| \leq \varepsilon_2 \quad (20)$$

3.4 Lyapunov Stability Analysis

All Consider a quadratic Lyapunov function [36] defined as:

$$V = \frac{1}{2}\left[\tilde{E}^2 + \tilde{I}^2 + \frac{1}{\kappa_1}\left(\hat{\Upsilon}_1 - \varepsilon_1\right)^2 + \frac{1}{\kappa_2}\left(\hat{\Upsilon}_2 - \varepsilon_2\right)^2\right] \quad (21)$$

Based on Equation (21), V is positive definite ($V \geq 0$).

Now, taking the derivative of V,

$$\dot{V} = \tilde{E}\dot{\tilde{E}} + \tilde{I}\dot{\tilde{I}} + \frac{1}{\kappa_1}\left(\hat{\Upsilon}_1 - \varepsilon_1\right)\dot{\hat{\Upsilon}}_1 + \frac{1}{\kappa_2}\left(\hat{\Upsilon}_2 - \varepsilon_2\right)\dot{\hat{\Upsilon}}_2 \quad (22)$$

By substituting (17) and (18) in to (22) following expression is obtained as

$$\begin{aligned}\dot{V} &= \tilde{E}\left[-\phi_1\tilde{E} - EX_1(S,\ E,\ I)\tilde{\theta}_1 - \hat{\Upsilon}_1 sgn\left(\tilde{E}\right)\right] + \frac{1}{\kappa_1}\left(\hat{\Upsilon}_1 - \varepsilon_1\right)\dot{\hat{\Upsilon}}_1 \\ &+ \tilde{I}\left[-\phi_2\tilde{I} - IX_2(S,\ E,\ I)\tilde{\theta}_2 - \hat{\Upsilon}_2 sgn(\tilde{I})\right] + \frac{1}{\kappa_2}\left(\hat{\Upsilon}_2 - \varepsilon_2\right)\dot{\hat{\Upsilon}}_2 \\ &= -\phi_1\tilde{E}^2 - \tilde{E}\left(EX_1(S,\ E,\ I)\tilde{\theta}_1\right) - \hat{\Upsilon}_1\tilde{E}sgn\left(\tilde{E}\right) + \frac{1}{\kappa_1}\left(\hat{\Upsilon}_1 - \varepsilon_1\right)\dot{\hat{\Upsilon}}_1 \\ &- \phi_2\tilde{I}^2 - \tilde{I}\left(IX_2(S,\ E,\ I)\tilde{\theta}_2\right) - \hat{\Upsilon}_2\tilde{I}sgn(\tilde{I}) + \frac{1}{\kappa_2}\left(\hat{\Upsilon}_2 - \varepsilon_2\right)\dot{\hat{\Upsilon}}_2\end{aligned} \quad (23)$$

Considering the fact that $\tilde{E}sgn\left(\tilde{E}\right) = \left|\tilde{E}\right|$ and $\tilde{I}sgn(\tilde{I}) = \left|\tilde{I}\right|$, and by substituting the adaptation laws defined in Equations (15) and (16),

$$\begin{aligned}\dot{V}(t) &= -\phi_1\tilde{E}^2 - \tilde{E}\left(EX_1(S,\ E,\ I)\tilde{\theta}_1\right) - \hat{\Upsilon}_1\left|\tilde{E}\right| + \frac{1}{\kappa_1}\left(\hat{\Upsilon}_1 - \varepsilon_1\right)\kappa_1\left|\tilde{E}\right| \\ &-\phi_2\tilde{I}^2 - \tilde{I}\left(IX_2(S,\ E,\ I)\tilde{\theta}_2\right) - \hat{\Upsilon}_2\left|\tilde{I}\right| + \frac{1}{\kappa_2}\left(\hat{\Upsilon}_2 - \varepsilon_2\right)\kappa_2\left|\tilde{I}\right|\end{aligned} \quad (24)$$

Given (19) and (20) and further simplification it is reduced to

$$\dot{V} = -\phi_1\tilde{E}^2 + \varepsilon_1\left|\tilde{E}\right| - \hat{\Upsilon}_1\left|\tilde{E}\right| + \frac{1}{\kappa_1}\left(\hat{\Upsilon}_1 - \varepsilon_1\right)\kappa_1\left|\tilde{E}\right| - \phi_2\tilde{I}^2 + \varepsilon_2\left|\tilde{I}\right| - \hat{\Upsilon}_2\left|\tilde{I}\right| + \frac{1}{\kappa_2}\left(\hat{\Upsilon}_2 - \varepsilon_2\right)\kappa_2\left|\tilde{I}\right|$$

$$\dot{V} = -\phi_1\tilde{E}^2 - \phi_2\tilde{I}^2 \leq 0 \quad (25)$$

Since λ_1 and λ_2 are positive constants, $\dot{V}$ is negative semi-definite ($\dot{V} \leq 0$). Hence, the designed adaptive control strategy given by (5.17) and (5.18) ensures the stability of the closed-loop tuberculosis control system. Moreover, employing the Barbalat's lemma [37] the asymptotic stability of the system may be proved by taking the derivative of (25)

$$\ddot{V} = -2\phi_1\tilde{E}\dot{\tilde{E}} - 2\phi_2\tilde{I}\dot{\tilde{I}} \quad (26)$$

Because of the boundedness of the exposed and infected dynamics (2) and (3), the derivatives $\dot{\text{E}}$ and $\dot{\text{I}}$ equally bounded. Considering the boundedness of $\dot{E}_r$, $\dot{\text{E}}$, $\dot{I}_r$ and $\dot{\text{I}}$, it can be established that $\dot{\tilde{E}}$ and $\dot{\tilde{I}}$ are bounded too. It emerges that $\ddot{V}$ is bounded based on the Barbalat's lemma $\left(\dot{V} \to 0\ as\ t \to \infty\right)$. Subsequently, the tracking errors converge ($\tilde{E} \to 0$ and $\tilde{I} \to 0$), which means the population of the exposed and infected converges to their reference trajectories ($E - E_r$ and $I \to I_r$), and hence the closed-loop tuberculosis control system is asymptotically stable regardless of parameter uncertainties.

4. Results and Discussion

Numerical simulation is conducted on the developed closed-loop TB control system, and the result is reported here. All the simulations are carried out using MATLAB 2019b software. The purpose of the simulation is

demonstrating the effectiveness of the developed control system and hence supports the established theoretical facts. In this regard, various simulation scenarios are considered. In the first instance, the nonlinear TB model is simulated without control; afterwards, the model is simulated along with the control inputs and predefined reference trajectories. In the second scenario, the capabilities of the adaptive control system to handle parameter uncertainties are shown.

The actual and estimated epidemiological parameters are given in Table 2. The actual parameters are assumed to be the same as the simulation parameters in [38]. For brevity, the estimated parameters are considered to contained 20% and 40% uncertainties as given in Equation (27) and (28), respectively.

That is,

$$\widehat{\boldsymbol{\theta}}_{\boldsymbol{20}} = 1.2\boldsymbol{\theta}_i \quad (27)$$

$$\widehat{\boldsymbol{\theta}}_{\boldsymbol{40}} = 1.4\boldsymbol{\theta}_i \quad (28)$$

for $i = 1, 2$

Where $\boldsymbol{\theta}$, $\widehat{\boldsymbol{\theta}}_{\boldsymbol{20}}$ and $\widehat{\boldsymbol{\theta}}_{\boldsymbol{40}}$ represents the actual model parameters, estimated parameters with 20% uncertainty and estimated parameters with 40% uncertainty, respectively.

Table 2. Simulation Parameters

Nominal parameter	**Value**	
$\boldsymbol{\theta_1} = [(1-\mathrm{p})\beta\ \mathrm{a}\ \mu]^{\mathrm{T}}$	$[0.0015\ \ 0.05\ \ 0.3]^{\mathrm{T}}$	
$\boldsymbol{\theta_2} = [\mathrm{p}\beta\ \mathrm{a}\ \mathrm{d}\ \mu]^{\mathrm{T}}$	$[0.0015\ \ 0.05\ \ 0.55\ \ 0.3]^{\mathrm{T}}$	
Uncertain parameter	$\hat{\theta}_{20}$	$\hat{\theta}_{40}$
$\widehat{\boldsymbol{\theta}}_{\boldsymbol{1}} = \left[(1-\hat{\mathrm{p}})\hat{\beta}\ \hat{\mathrm{a}}\ \hat{\mu}\right]^{\mathrm{T}}$	$[0.0018\ \ 0.06\ \ 0.36]^{\mathrm{T}}$	$[0.0021\ \ 0.07\ \ 0.42]^{\mathrm{T}}$
$\widehat{\boldsymbol{\theta}}_{\boldsymbol{2}} = \left[\hat{\mathrm{p}}\hat{\beta}\ \hat{\mathrm{a}}\ \ \hat{\mathrm{d}}\ \hat{\mu}\right]^{\mathrm{T}}$	$[0.0018\ \ 0.06\ \ 0.66\ \ 0.36]^{\mathrm{T}}$	$[0.0021\ \ 0.07\ \ 0.77\ \ 0.42]^{\mathrm{T}}$

The reference trajectories for the reduction of the exposed and infected individuals (E_r, I_r) are designed as descending exponential functions to mimic a planned tuberculosis control intervention program that aimed at eliminating the tuberculosis epidemic by reducing the number of the exposed and infected population to zero. The reference trajectories over control program period t are defined as:

$$E_r = \left(E_0 - E_f\right)e^{-\epsilon_1 t} + E_f \quad (29)$$

$$I_r = \left(I_0 - I_f\right)e^{-\epsilon_2 t} + I_f \quad (30)$$

Where E_0, E_f, I_0, and I_f represents the initial and final values of the exposed and infected population. The desired steady-state (final) number of the exposed and infected individuals are considered to be zero i.e. $E_f = I_f = 0$, $\epsilon_1 = 0.5$, $\epsilon_1 = 0.5$, $\epsilon_2 = 0.4$, and the control program period $t = 15$. Figure 3 shows the desired trajectories for the specified parameters. As shown in the figure, the decrease in the number of exposed is more gradual compared to the infected, since the spread of the disease can be better handle if the number of infected are eliminated faster then followed by the exposed.

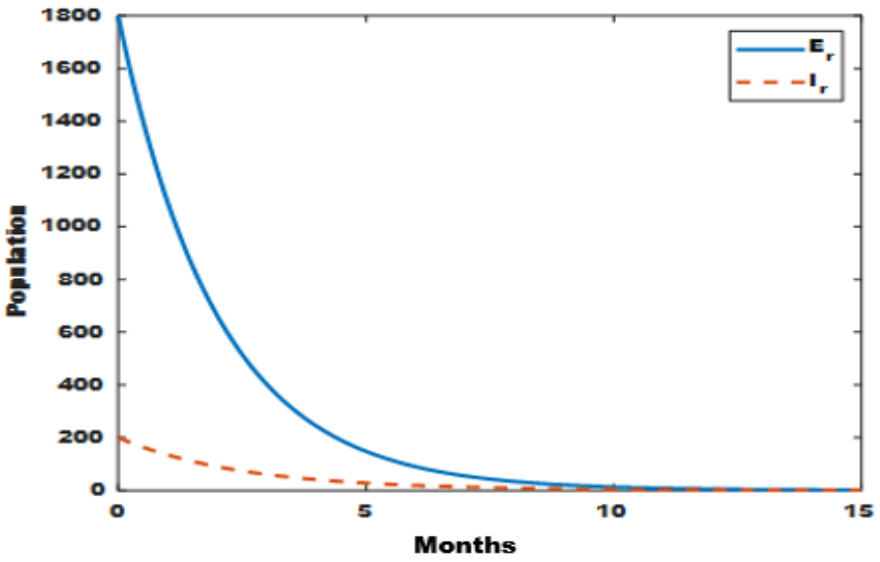

Figure 3. Control reference signals

Figure 4 shows the trajectories of the susceptible, exposed and infected populations when there is no control intervention (control inputs $u_1 = u_2 = 0$). It can be vividly observed that the number of healthy susceptible people decreases while the population of the exposed and infected are increasing. This means there is an epidemic and the disease remain in the community. This undesirable situation can be averted by employing appropriate controls.

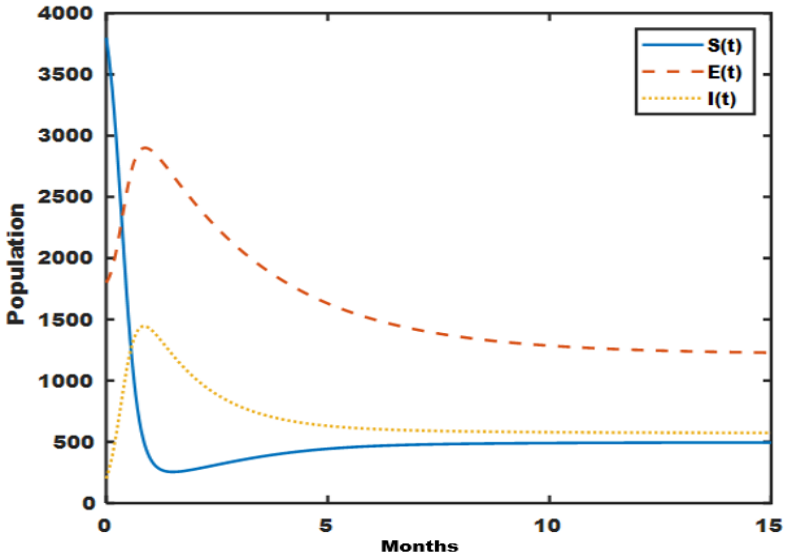

Figure 4. Dynamics of TB without control

Afterwards, the closed-loop system along with the adaptive control inputs $u_1(t)$ and $u_2(t)$ is simulated using the actual system parameters, and desired reference values of the exposed and infected individuals (see Figure 5). The controller parameters are adjusted to $\phi_1 = \phi_2 = 48$, $\Upsilon_{10} = \Upsilon_{20} = 2$, $\kappa_1 = 0.2$ and $\kappa_2 = 1$ to accomplish a high rate of convergence of the tracking errors with a settling time $t_{SE} = 0.6522$ and $t_{SI} = 0.5435$ for the exposed and infectious, respectively. Furthermore, it can be seen from Figure 4, that there is high accuracy in the tracking of the descending reference trajectories of the exposed and infected population. The mean absolute tracking error (MAE) for the exposed and infectious trajectories is found to be equal to 0.080954 and 0.00002 respectively.

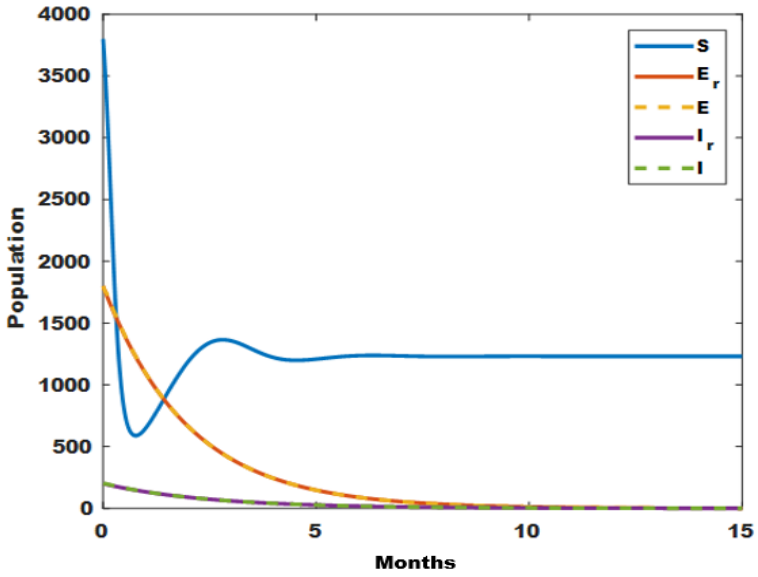

Figure 5. Closed-loop TB control system with adaptive control inputs

For the purpose of comparison, the performance of the adaptive controller in handling the effect of the parameter uncertainties is compared with the optimal controller designed in chapter four. In this scenario, the optimal trajectories of the exposed and infected individuals obtained from the optimal controller in [38], are used as reference inputs (E_r, I_r). Figures 5 and 6 show the resulting dynamics of the exposed and infected individuals in case of the TB control system with adaptive control and the TB model with conventional optimal control in the presence of 20% and 40% uncertainties.

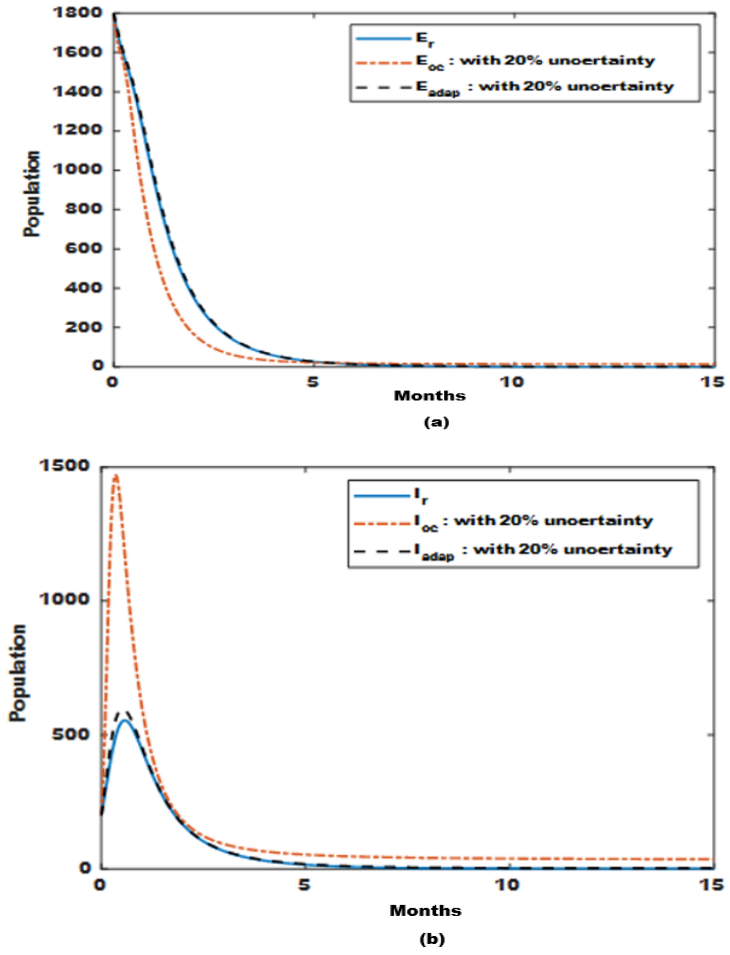

Figure 6. Effect of 20% uncertainty in the estimated model parameters: (a) Exposed population (b) Infectious population

As shown in Figure 6 and 7, in the presence of parameter uncertainties, the performance of the conventional optimal controller is affected and the trajectories of both the exposed and infectious population deviated from the reference trajectories. The mean absolute tracking error (MAE), for the optimal controller in the presence of 20% uncertainty is 51.2283 and 69.1930 for the exposed and infectious trajectories, and is found to be equal to 71.0222, 102.8563 in the presence of 40% uncertainty. Besides, the result of the adaptive controller demonstrated the robustness of the controller in handling the parametric uncertainties, with MAE of 0.8494, and 0.7357 for the exposed and infectious under 20% uncertainty, and 0.9332 and 1.0780 in the presence of 40% uncertainty. Hence, the adaptive controller successfully tracks the reference trajectories of the exposed and infectious population.

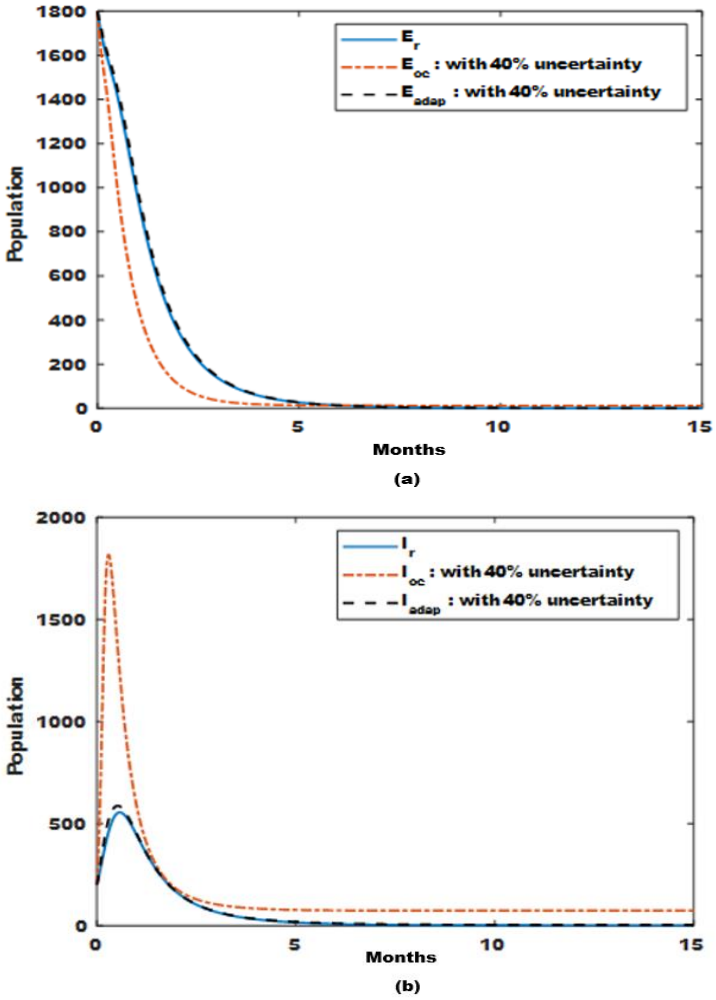

Figure 7. Effect of 40% uncertainty in the estimated model parameters: (a) Exposed population (b) Infectious population

5. Conclusion

The study presented the analysis of adaptive sliding mode control for non-linear TB dynamic model, by considering system parameter uncertainties. The goal of the control was to reduce the population of individuals that are exposed and infected to zero by tracking a predefined reference trajectory. Adaption law is established to update the parameter values to ensure the robustness of the control system against uncertainties. The stability of the closed-loop system is demonstrated using the Lyapunov Function Principle, and the analytical analysis was supported with a numerical simulation. The conclusion suggested that the proposed adaptive control systems are very useful and provide efficient tools for understanding TB transmission and control. The adaptive control system is robust against the various level of uncertainties and ensures the convergence of the number of exposed and infectious individuals to the desired values. The research presents a novel Robust Adaptive Sliding Mode Control approach for managing TB under parameter uncertainties. By integrating control system theory, Lyapunov stability analysis, and numerical simulations, it

enhances understanding of disease dynamics and control strategies. The study's insights can inform the development of more effective control programs to combat infectious diseases like TB, aligning with global health objectives for disease eradication.

The procedure of development and analysis of mathematical epidemic models is complex and quite challenging. Meanwhile, recent studies revealed that the application of data-driven methods such as machine learning algorithms could alternatively produce accurate epidemic predictive models. Because there is increased in computational power, the use of machine learning algorithms in epidemiology is promising and future study would consider the data-driven approach. Another important control method to be considered is the intelligent control systems design using direct and indirect neural network controllers and Fuzzy controllers.

6. References

[1] P. Di Giamberardino and D. Iacoviello, "Modeling and control of an epidemic disease under possible complication," *2018 22nd Int. Conf. Syst. Theory, Control Comput.*, pp. 67–72, 2018.

[2] H. Heesterbeek *et al.*, "Modeling infectious disease dynamics in the complex landscape of global health," *Science (80-.).*, vol. 347, no. 6227, p. aaa4339, 2015, doi: 10.1126/science.aaa4339.

[3] C. H. Li, "Dynamics of a network-based SIS epidemic model with nonmonotone incidence rate," *Phys. A Stat. Mech. its Appl.*, vol. 427, pp. 234–243, 2015, doi: 10.1016/j.physa.2015.02.023.

[4] J. Jumbo, D. O. Obaseki, and P. O. Ikuabe, "Tuberculosis and gender parity in a TB Referral Centre, South –South Nigeria," *Greener J. Med. Sci.*, vol. 3, no. 7, pp. 270–275, 2013, doi: 10.15580/gjms.2013.7.082613801.

[5] E. M. Rocha, C. J. Silva, and D. F. M. Torres, "The effect of immigrant communities coming from higher incidence tuberculosis regions to a host country," *Ric. di Mat.*, vol. 67, no. 1, pp. 89–112, 2018, doi: 10.1007/s11587-017-0350-z.

[6] C. P. Bhunu, "Mathematical analysis of a three-strain tuberculosis transmission model," *Appl. Math. Model.*, vol. 35, no. 9, pp. 4647–4660, 2011, doi: 10.1016/j.apm.2011.03.037.

[7] M. G. M. Gomes *et al.*, "Implications of partial immunity on the prospects for tuberculosis control by post-exposure interventions," vol. 248, pp. 608–617, 2007, doi: 10.1016/j.jtbi.2007.06.005.

[8] P. Chaulet, "Treatment of tuberculosis: case holding until cure (No. WHO/TB/83.141 Rev. 2. Unpublished).," 1983.

[9] G. Yang, P. Cao, X. Wang, and D. He, "Modelling the Measles Outbreak at Hong Kong International Airport in 2019: A Data-Driven Analysis on the Effects of Timely Reporting and Public Awareness," *Infect. Drug Resist.*, vol. 13, no. 6, pp. 1851–1861, 2020, doi: 10.2147/IDR.S258035.

[10] Q. Lin, S. Zhao, D. Gao, Y. Lou, S. Yang, and S. S. Musa, "A conceptual model for the outbreak of Coronavirus disease 2019 (COVID-19) in Wuhan, China with individual reaction and governmental action," *Int. J. Infect. Dis.*, vol. 93, no. 61373005, pp. 211–216, 2020, doi: 10.1016/j.ijid.2020.02.058.

[11] H. Sofia, M. T. T. Monteiro, and D. F. M. Torres, "Coexistence of two dengue virus serotypes and forecasting for Madeira Island," *Oper. Res. Heal. Care*, vol. 7, pp. 122–131, 2015, doi: 10.1016/j.orhc.2015.07.003.

[12] S. J. Gambhire, D. R. Kishore, P. S. Londhe, and S. N. Pawar, "Review of sliding mode based control techniques for control system applications," *Int. J. Dyn. Control*, 2020, doi: 10.1007/s40435-020-00638-7.

[13] M. Djouima, A. T. Azar, S. Drid, and D. Mehdi, "Higher Order Sliding Mode Control for Blood Glucose Regulation of Type 1 Diabetic Patients," *Int. J. Syst. Dyn. Appl.*, vol. 7, no. 1, pp. 65–84, 2017, doi: 10.4018/ijsda.2018010104.

[14] Windarto and N. Anggriani, "Global stability for a susceptible-infectious epidemic model with fractional incidence rate," *Appl. Math. Sci.*, vol. 9, no. 73–76, pp. 3775–3788, 2015, doi: 10.12988/ams.2015.54294.

[15] J. S. Lopes, P. Rodrigues, S. T. R. Pinho, R. F. S. Andrade, R. Duarte, and M. G. M. Gomes, "Interpreting measures of tuberculosis transmission: A case study on the Portuguese population," *BMC Infect. Dis.*, vol. 14, no. 1, pp. 1–9, 2014, doi: 10.1186/1471-2334-14-340.

[16] N. Yi, Q. Zhang, K. Mao, D. Yang, and Q. Li, "Analysis and control of an SEIR epidemic system with nonlinear transmission rate," *Math. Comput. Model.*, vol. 50, no. 9–10, pp. 1498–1513, 2009, doi: 10.1016/j.mcm.2009.07.014.

[17] B. Matthew and J. Keeling, *Modeling Infectious Diseases in Humans and Animals Diseases in Humans*.

USA: Princeton, NJ: Princeton University Press, 2008.

[18] S. R. Gani and S. V Halawar, "Optimal control for the spread of infectious disease: The role of awareness programs by media and antiviral treatment," *Optim. Control Appl. Methods*, vol. 39, no. 4, pp. 1407–1430, 2018, doi: 10.1002/oca.2418.

[19] C. Chen, Y. Ding, X. Wen, B. Wang, L. Gao, and K. Tan, "Optimal control nodes in disease-perturbed networks as targets for combination therapy," *Nat. Commun.*, vol. 10, no. 2180, pp. 1–14, 2019, doi: 10.1038/s41467-019-10215-y.

[20] F. T. Saad and E. Hincal, "An optimal control approach for the interaction of immune checkpoints, immune system, and BCG in the treatment of superficial bladder cancer," *Eur. Phys. J. Plus*, vol. 133, no. J241, pp. 1–14, 2018, doi: 10.1140/epjp/i2018-12092-0.

[21] A. G. Lambura, G. G. Mwanga, and L. Luboobi, "Mathematical Model for Optimal Control of Soil-Transmitted Helminth Infection," *Comput. Math. Methods Med.*, vol. 2020, pp. 1–15, 2020.

[22] D. Yaro, W. Osafo, A. Saviour, W. Akuamoah, and D. Lu, "Analysis and Optimal Control of Fractional-Order Transmission of a Respiratory Epidemic Model," *Int. J. Appl. Comput. Math.*, vol. 5, no. 4, pp. 1–21, 2019, doi: 10.1007/s40819-019-0699-7.

[23] A. El, A. Laaroussi, R. Ghazzali, M. Rachik, and S. Benrhila, "Modeling the spatiotemporal transmission of Ebola disease and optimal control : a regional approach," *Int. J. Dyn. Control*, vol. 7, no. 3, pp. 1110–1124, 2019, doi: 10.1007/s40435-019-00525-w.

[24] D. Khamis, C. El Mouden, K. Kura, and M. B. Bonsall, "Optimal control of malaria : combining vector interventions and drug therapies," *Malar. J.*, vol. 17, no. 74, pp. 1–18, 2018, doi: 10.1186/s12936-018-2321-6.

[25] M. K. Bera, P. Kumar, and R. K. Biswas, "Robust control of HIV infection by antiretroviral therapy : a super-twisting sliding mode control approach," *IET Syst. Biol.*, no. 1, pp. 1–9, 2019.

[26] A. Rajaei, A. Vahidi-Moghaddam, A. Chizfahm, and M. Sharifi, "Control of malaria outbreak using a non-linear robust strategy with adaptive gains," *IET Control Theory Appl.*, vol. 13, no. 14, pp. 2308–2317, 2019, doi: 10.1049/iet-cta.2018.5292.

[27] O. Aghajanzadeh, M. Sharifi, S. Tashakori, and H. Zohoor, "Nonlinear adaptive control method for treatment of uncertain hepatitis B virus infection," *Biomed. Signal Process. Control*, vol. 38, no. September, pp. 174–181, 2017, doi: 10.1016/j.bspc.2017.06.008.

[28] C. Y. Chen and G. T. C. Chiu, "H∞ robust controller design of media advance systems with time domain specifications," *Int. J. Innov. Comput. Inf. Control*, vol. 4, no. 4, pp. 813–828, 2008.

[29] S. Tong, W. Wang, and L. Qu, "Decentralized robust control for uncertain T-S fuzzy large-scale systems with time-delay," *Int. J. Innov. Comput. Inf. Control*, vol. 3, no. 3, pp. 657–672, 2007.

[30] M. S. Gaya, N. A. Wahab, Y. Sam, and S. I. Samsuddin, "Comparison of ANFIS and Neural Network Direct Inverse Control Applied to Wastewater Treatment System," vol. 845, pp. 543–548, 2014, doi: 10.4028/www.scientific.net/AMR.845.543.

[31] J. Khodaei-mehr, S. Tangestanizadeh, R. Vatankhah, and M. Sharifi, "ANFIS-Based Optimal Control of Hepatitis C virus epidemic," *IFAC-PapersOnLine*, vol. 51, no. 15, pp. 539–544, 2018, doi: 10.1016/j.ifacol.2018.09.211.

[32] C. C. Mccluskey, "Lyapunov Functions for Tuberculosis Models with Fast and Slow Progression," 2006.

[33] A. Ibeas, M. De La Sen, and S. Alonso-Quesada, "Robust sliding control of SEIR epidemic models," *Math. Probl. Eng.*, vol. 2014, pp. 1–11, 2014, doi: 10.1155/2014/104764.

[34] P. Taylor, F. Plestan, Y. Shtessel, V. Brégeault, and A. Poznyak, "New methodologies for adaptive sliding mode control," *Int. J. Control*, vol. 83, no. 9, pp. 1907–1919, 2010, doi: 10.1080/00207179.2010.501385.

[35] M. Sharifi and H. Moradi, "Nonlinear robust adaptive sliding mode control of influenza epidemic in the presence of uncertainty," *J. Process Control*, vol. 56, no. August, pp. 48–57, 2017, doi: 10.1016/j.jprocont.2017.05.010.

[36] H. Moradi, M. Sharifi, and G. Vossoughi, "Adaptive robust control of cancer chemotherapy in the presence of parametric uncertainties: A comparison between three hypotheses," *Comput. Biol. Med.*, vol. 56, no. November, pp. 145–157, 2015, doi: 10.1016/j.compbiomed.2014.11.002.

[37] J.-J. E. Slotine and W. Li, *Applied Nonlinear Control*. Englewood Cliffs, NJ: Prentice hall, 1991.

[38] R. A. Abdulkadir and P. Esmaili, "Optimal Control Cost-Effectiveness Analysis of Tuberculosis Model With Fast And Slow Progression," *Int. Trans. J. Eng. Manag. Appl. Sci. Technol.*, vol. 11, no. 7, pp. 1–13, 2020, doi: 10.14456/ITJEMAST.2020.131.